



Supplement of

The impact of aerosol size-dependent hygroscopicity and mixing state on the cloud condensation nuclei potential over the north-east Atlantic

Wei Xu et al.

Correspondence to: Ru-Jin Huang (rujin.huang@ieecas.cn) and Colin O'Dowd (colin.odowd@nuigalway.ie)

The copyright of individual parts of the supplement might differ from the article licence.

Content

Table S1. The arithmetic mean (standard deviation) of predicted N_{CCN} by each method in different types of air masses.

Figure S1. Sea surface Chlorophyll concentration during high biological activity period (top) and low biological activity period (bottom) for the year 2009 to 2010 in the North Atlantic Ocean. The monthly sea surface chlorophyll-a concentration data were downloaded from the EU Copernicus Marine Environment Monitoring Service (<http://marine.copernicus.eu/>) based on a multisensory approach.

Figure S2. The frequency distribution of 96 hours HYSPLIT backward trajectories ending at 100 meter height at Mace Head for each principal sector with colour codes representing frequency of the trajectories passing through the specific location.

Figure S3. The normalised wind rose plot (top) for each air mass with colour codes representing the frequency of occurrence; the boxplots represent black carbon, number of particles larger than 30 nm (N_{30}) (middle); air temperature, mean sea level pressure, precipitation, and relative humidity in each air mass (bottom). The horizontal lines represent median value, boxes represent 25th to 75th quantile, whiskers represent 1.5 inter-quarter range and markers represent outliers.

Figure S4. Comparison of measured N_{CCN} against estimated N_{CCN} under different SS using each method in Mixed-L and Mixed-H. The colour codes represent SS, equation of regression line, Pearson correlation efficient and relative root square error (RRSE) are shown in each panel. The dashed lines represent 30% uncertainty ranges. To note that axes are in logarithmic scales.

Figure S5. The normalised frequency of distribution of critical diameter (D_{crit} , nm) obtained by method A (chemical composition) for different types of air masses.

Figure S6. The normalised frequency of distribution of critical diameter (D_{crit} , nm) obtained by method D (size dependent growth factor) for different types of air masses.

Figure S7. Size resolved activation fraction obtained by method F (growth factor- probability density function, GF-PDF) for different types of air masses. The lines represent median activation fractions, the shaded area represents 25th to 75th percentiles. The colours represent different supersaturations(SS).

Figure S8. The size resolved number fractions of near-hydrophobic (NH, blue), more-hygroscopic (MH, red) and sea-salt (SS, orange) modes for different types of air mass used in method D.

Figure S9. The averaged growth-factor probability density function for different types of air masses.

Table S1. The arithmetic mean (standard deviation) of predicted N_{CCN} by each method in different types of air masses.

sector	supersaturation	A	B	C	D	E	F
Clean-H	0.25% SS	97(43)	115(53)	110(48)	107(47)	107(47)	106(47)
	0.5% SS	146(88)	212(125)	212(118)	170(97)	176(101)	173(98)
	0.75% SS	211(127)	326(177)	346(177)	287(155)	287(154)	279(150)
	1% SS	424(199)	539(272)	556(282)	505(254)	502(253)	495(248)
Clean-L	0.25% SS	143(79)	171(100)	162(90)	156(87)	155(87)	153(85)
	0.5% SS	202(130)	294(186)	279(172)	224(149)	228(151)	223(146)
	0.75% SS	289(186)	422(238)	430(238)	337(211)	340(211)	333(207)
	1% SS	373(219)	474(271)	486(277)	412(247)	406(248)	399(243)
Mix-H	0.25% SS	233(157)	267(175)	249(162)	231(149)	227(146)	224(141)
	0.5% SS	371(293)	448(329)	435(327)	365(271)	359(260)	354(253)
	0.75% SS	491(388)	593(418)	597(426)	504(370)	497(360)	488(352)
	1% SS	620(491)	706(522)	728(551)	625(461)	616(457)	603(446)
Mix-L	0.25% SS	679(767)	752(858)	636(737)	595(716)	570(698)	559(691)
	0.5% SS	1041(1221)	1129(1267)	1023(1196)	925(1141)	897(1133)	870(1112)
	0.75% SS	1267(1426)	1385(1480)	1298(1423)	1174(1361)	1152(1361)	1114(1341)
	1% SS	1405(1638)	1504(1655)	1419(1568)	1279(1507)	1255(1498)	1214(1478)
Polluted-H	0.25% SS	564(418)	601(416)	538(376)	485(351)	467(334)	455(322)
	0.5% SS	1019(691)	1096(673)	1036(642)	869(587)	833(558)	804(522)
	0.75% SS	1335(827)	1424(817)	1411(808)	1210(728)	1152(708)	1114(656)
	1% SS	1604(858)	1668(843)	1689(842)	1477(752)	1436(744)	1351(687)
Polluted-L	0.25% SS	1465(1039)	1442(1034)	1154(922)	1061(889)	975(863)	952(848)
	0.5% SS	2343(1530)	2309(1463)	2040(1355)	1793(1308)	1692(1287)	1608(1251)
	0.75% SS	2830(1768)	2825(1685)	2622(1601)	2328(1555)	2244(1539)	2108(1482)
	1% SS	3379(2188)	3322(1929)	3141(1861)	2834(1790)	2768(1785)	2583(1722)

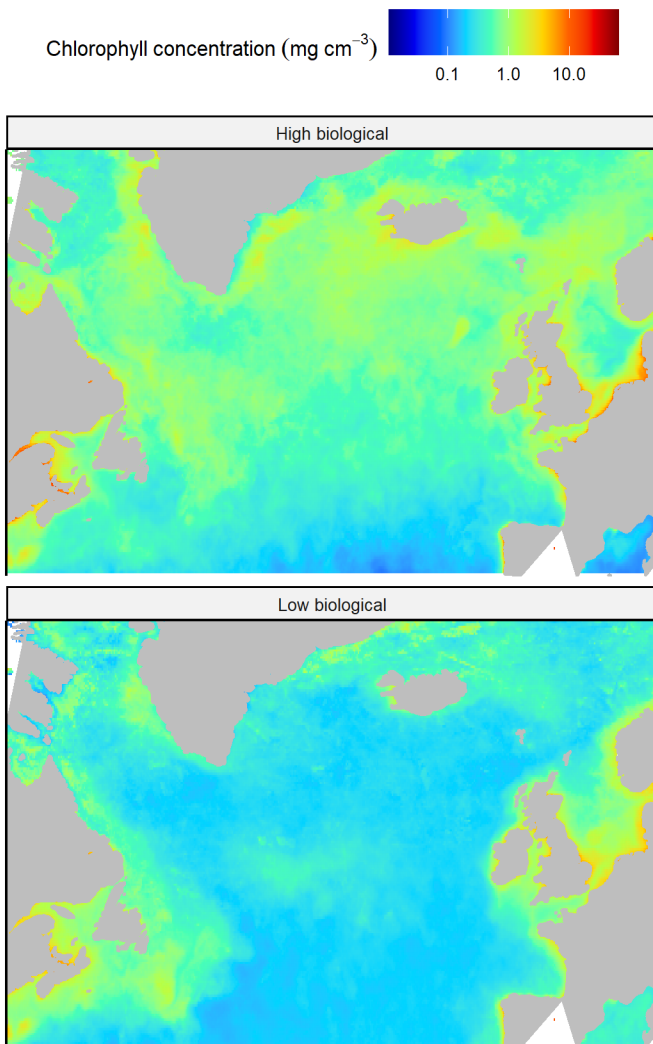


Figure S1. Sea surface Chlorophyll concentration during high biological activity period (top) and low biological activity period (bottom) for the year 2009 to 2010 in the North Atlantic Ocean. The monthly sea surface chlorophyll-a concentration data were downloaded from the EU Copernicus Marine Environment Monitoring Service (<http://marine.copernicus.eu/>) based on a multisensory approach.

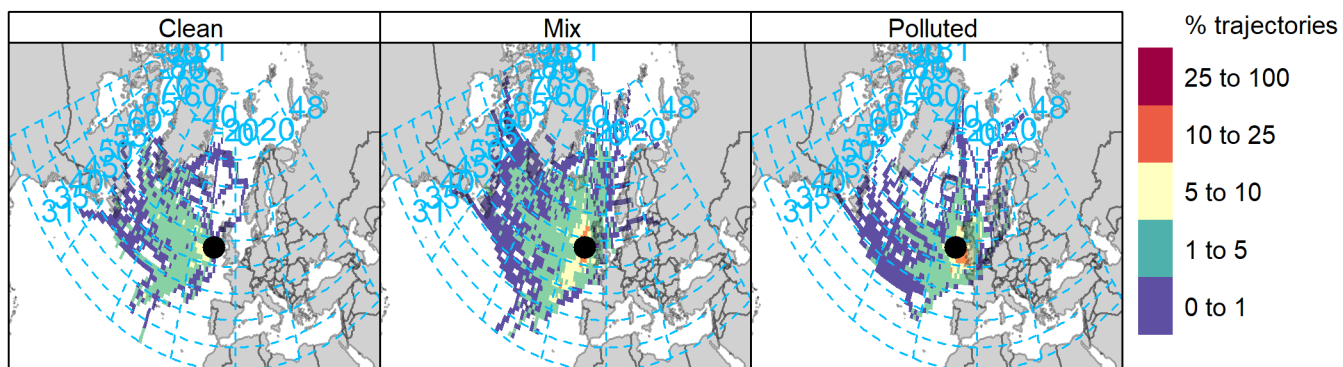


Figure S2. The frequency distribution of 96 hours HYSPLIT backward trajectories ending at 100 meter height at Mace Head for each principal sector, colour codes represent frequency of the trajectories passing through the specific location.

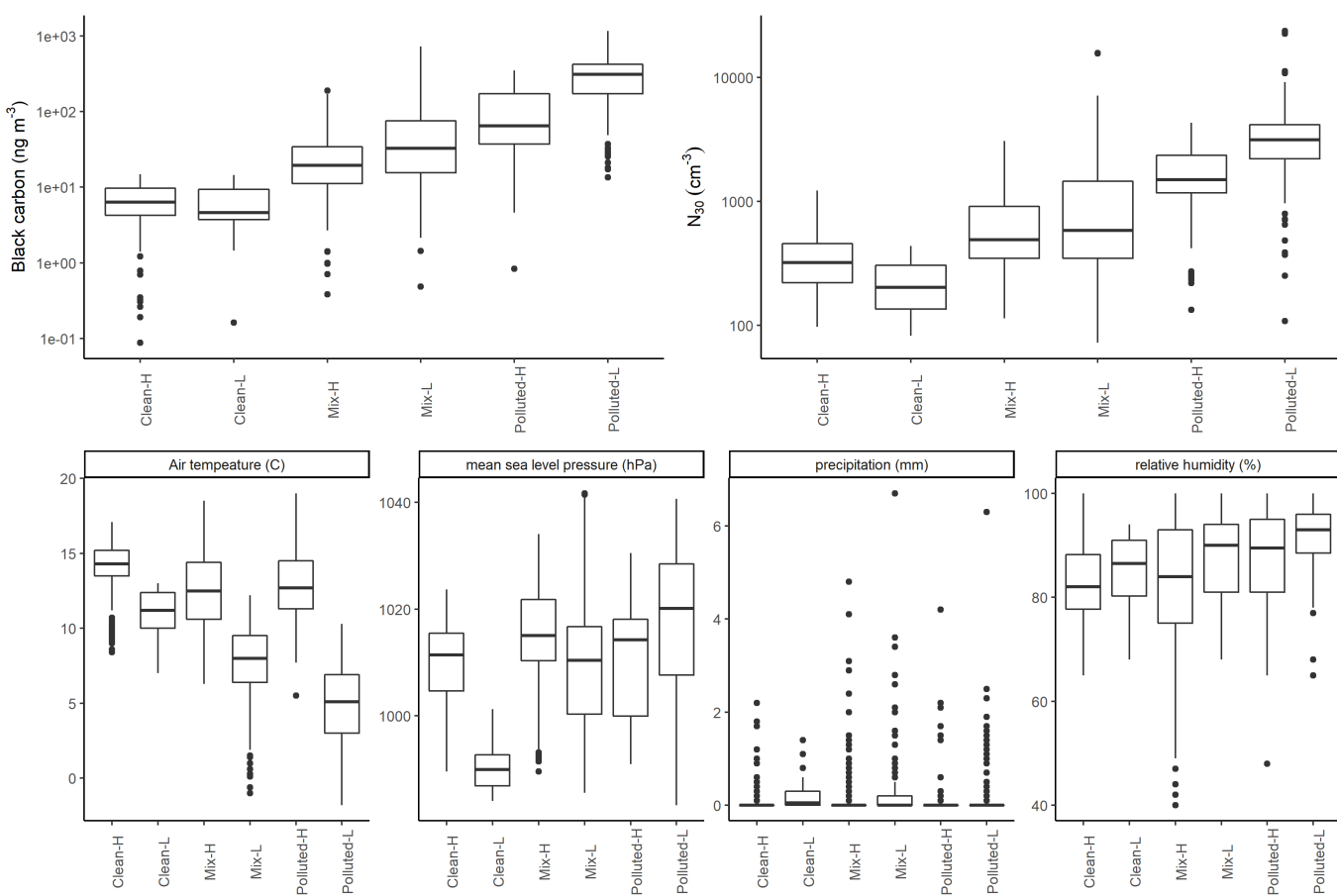
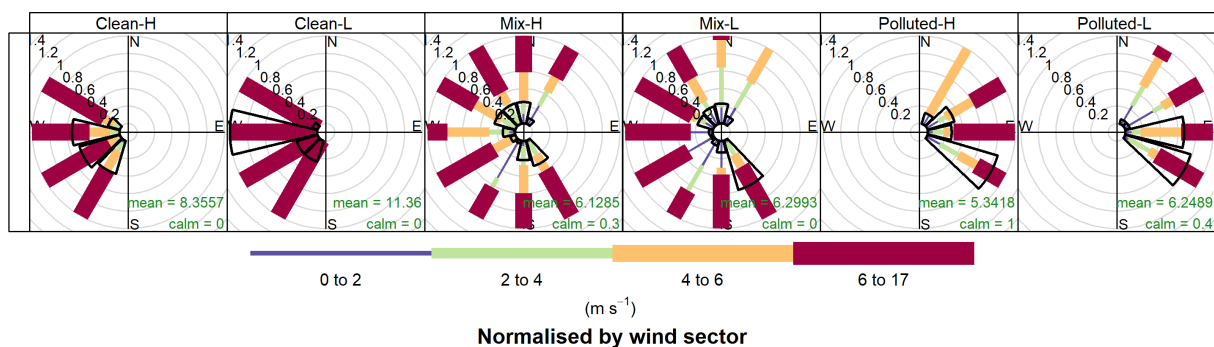


Figure S3. The normalised wind rose plot (top) for each air mass with colour codes representing the frequency of occurrence; the boxplots represent black carbon, number of particles larger than 30 nm (N₃₀) (middle); air temperature, mean sea level pressure, precipitation, and relative humidity in each air mass (bottom). The horizontal lines represent median value, boxes represent 25th to 75th quantile, whiskers represent 1.5 inter-quarter range and markers represent outliers.

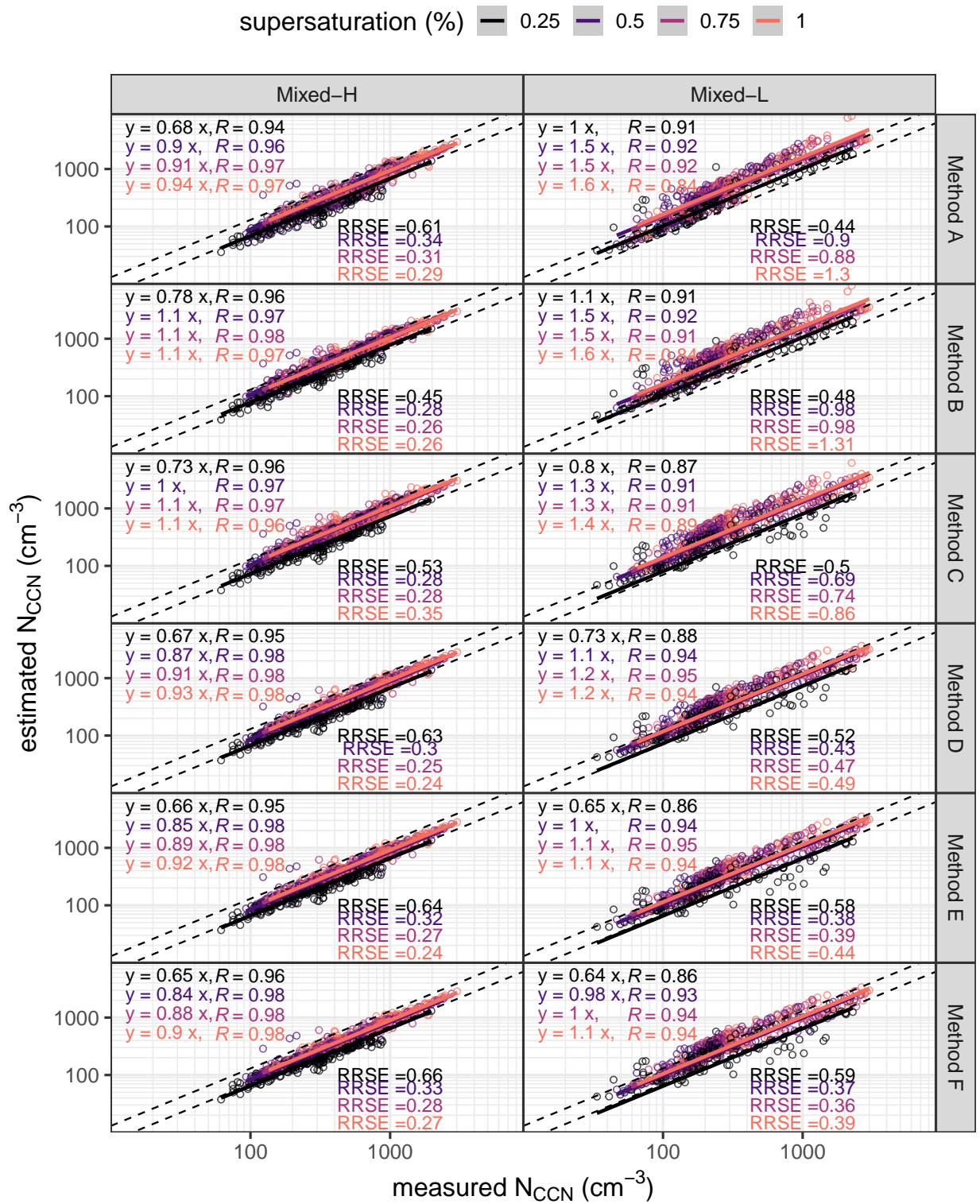


Figure S4. Comparison of measured NCCN against estimated NCCN under different SS using each method in Mixed-L and Mixed-H. The colour codes represent SS, equation of regression line, Pearson correlation efficient and relative root square error (RRSE) are shown in each panel. The dashed lines represent 30% uncertainty ranges. To note that axes are in logarithmic

scales.

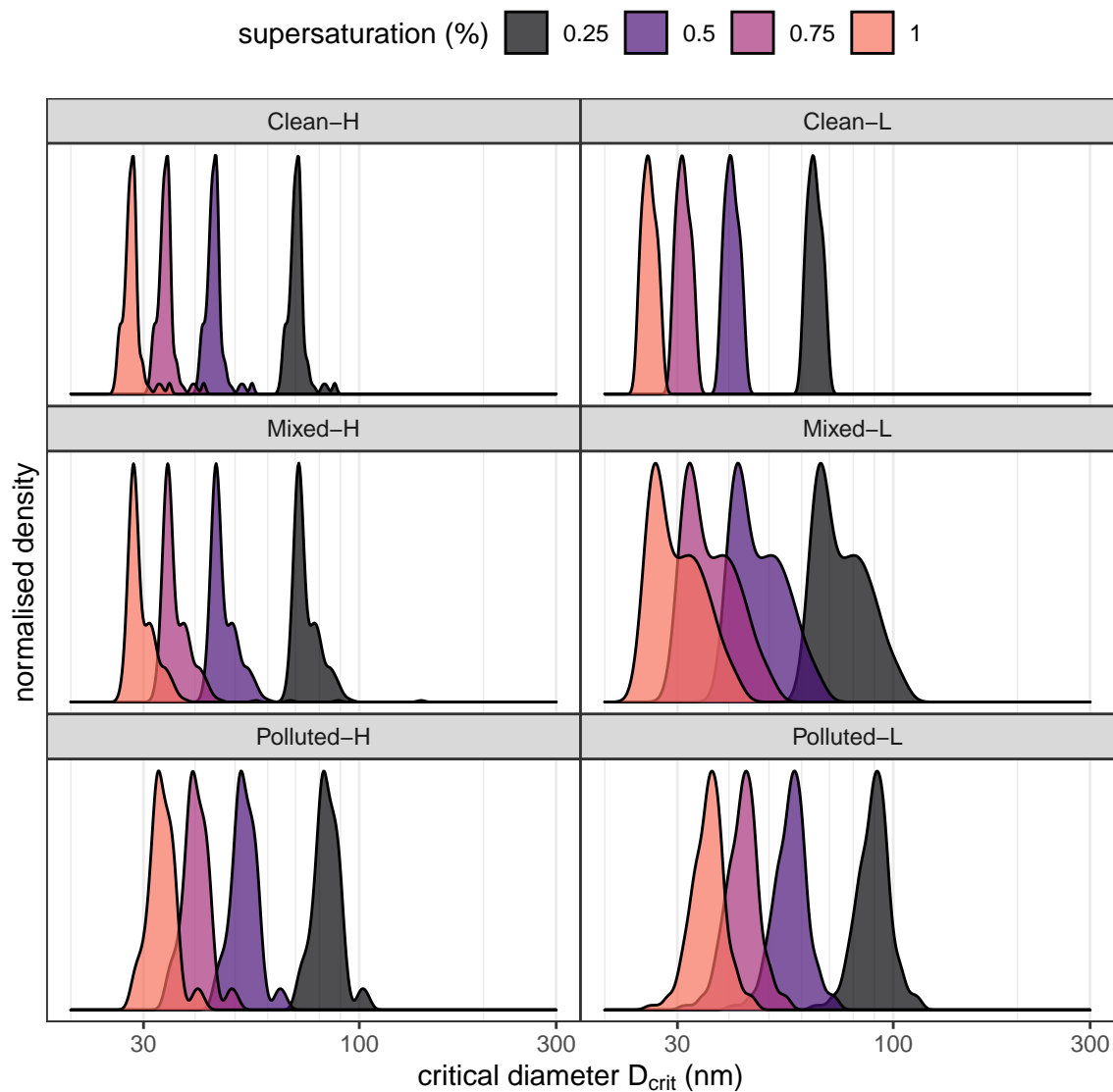


Figure S5. The normalised frequency of distribution of critical diameter (D_{crit} , nm) obtained by method A (chemical composition) for different types of air masses.

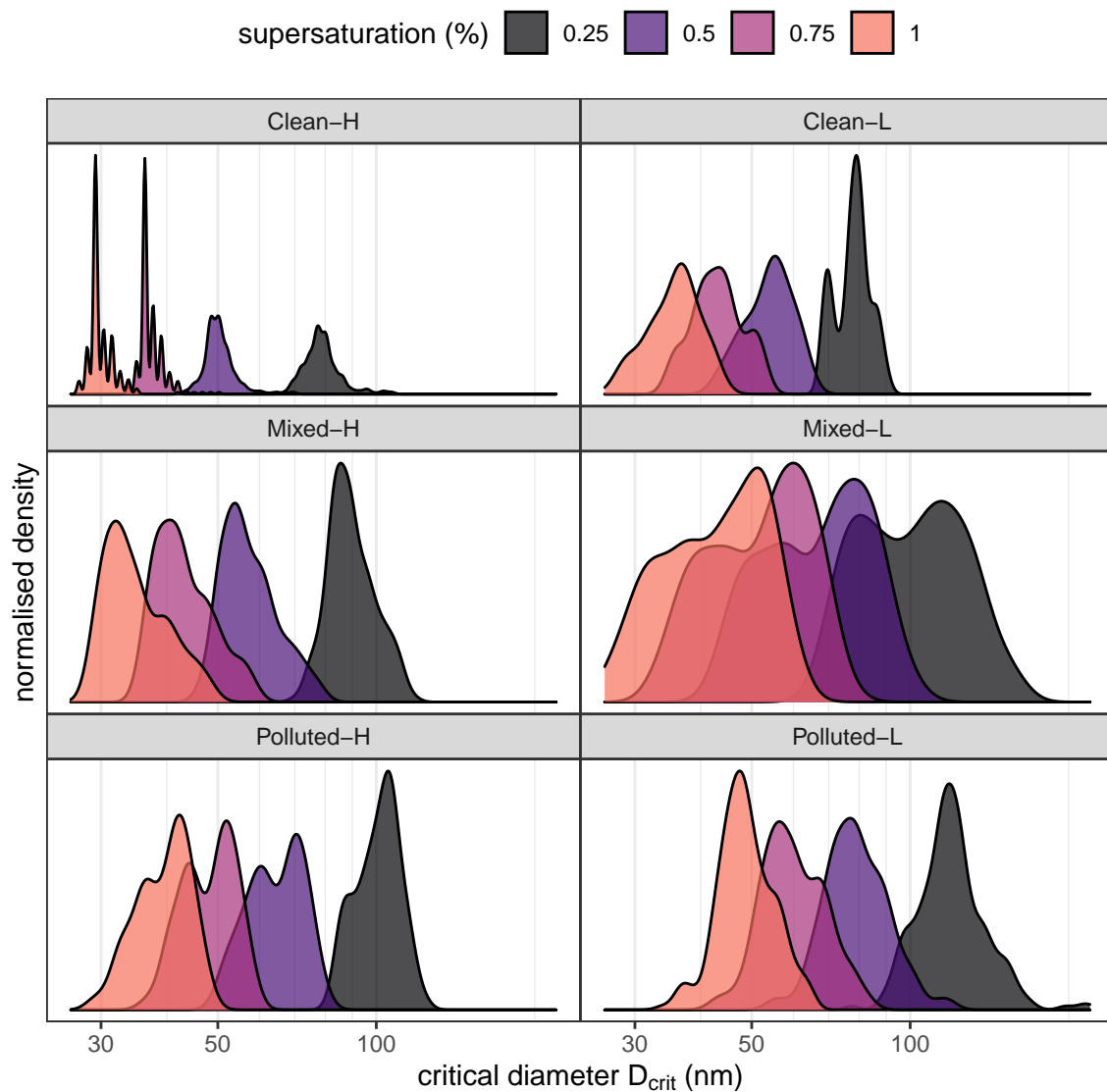


Figure S6. The normalised frequency of distribution of critical diameter (D_{crit} , nm) obtained by method D (size dependent growth factor) for different types of air masses.

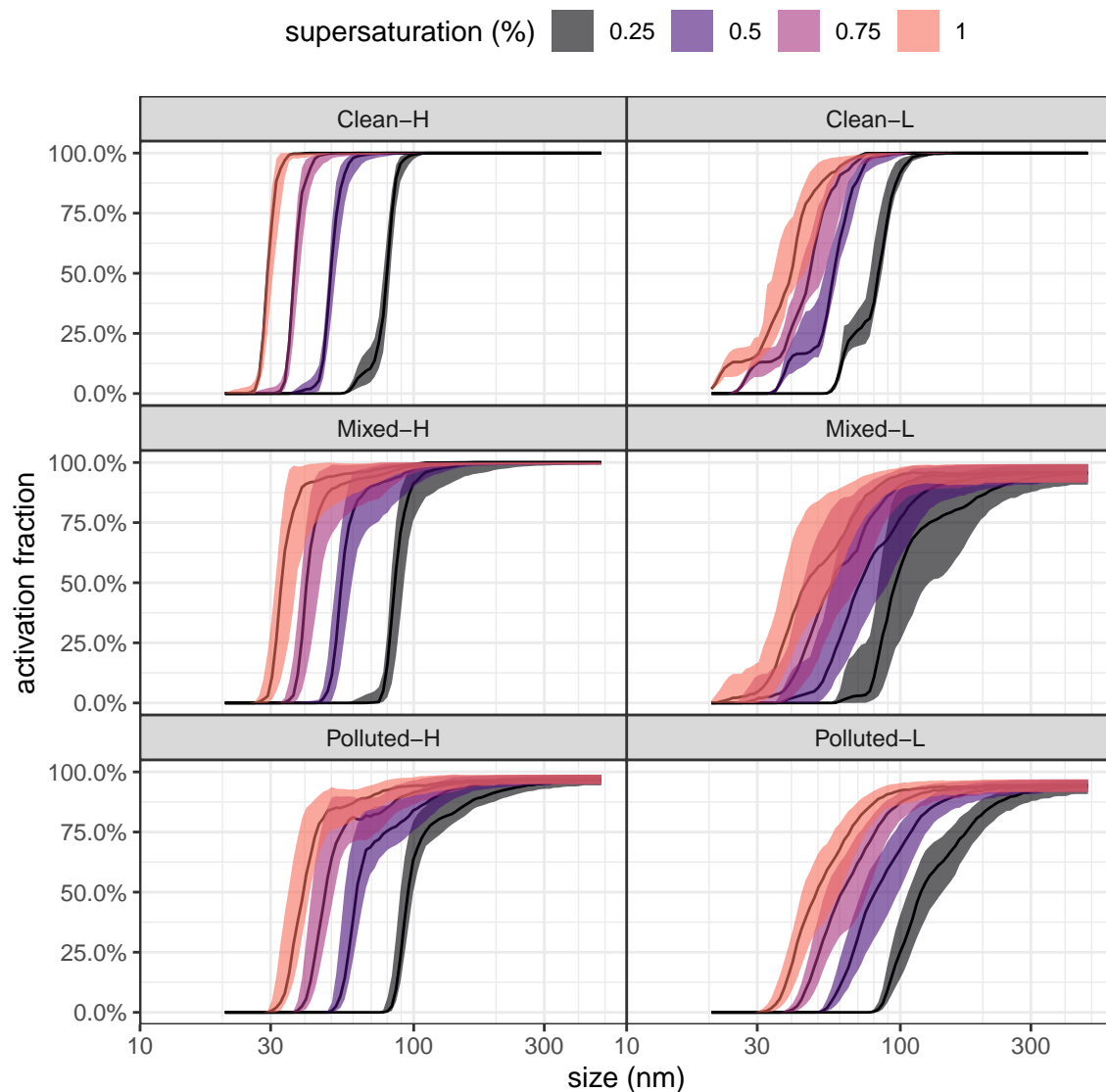


Figure S7. Size resolved activation fraction obtained by method F (growth factor- probability density function, GF-PDF) for different types of air masses. The lines represent median activation fractions, the shaded area represents 25th to 75th percentiles. The colours represent different supersaturations.

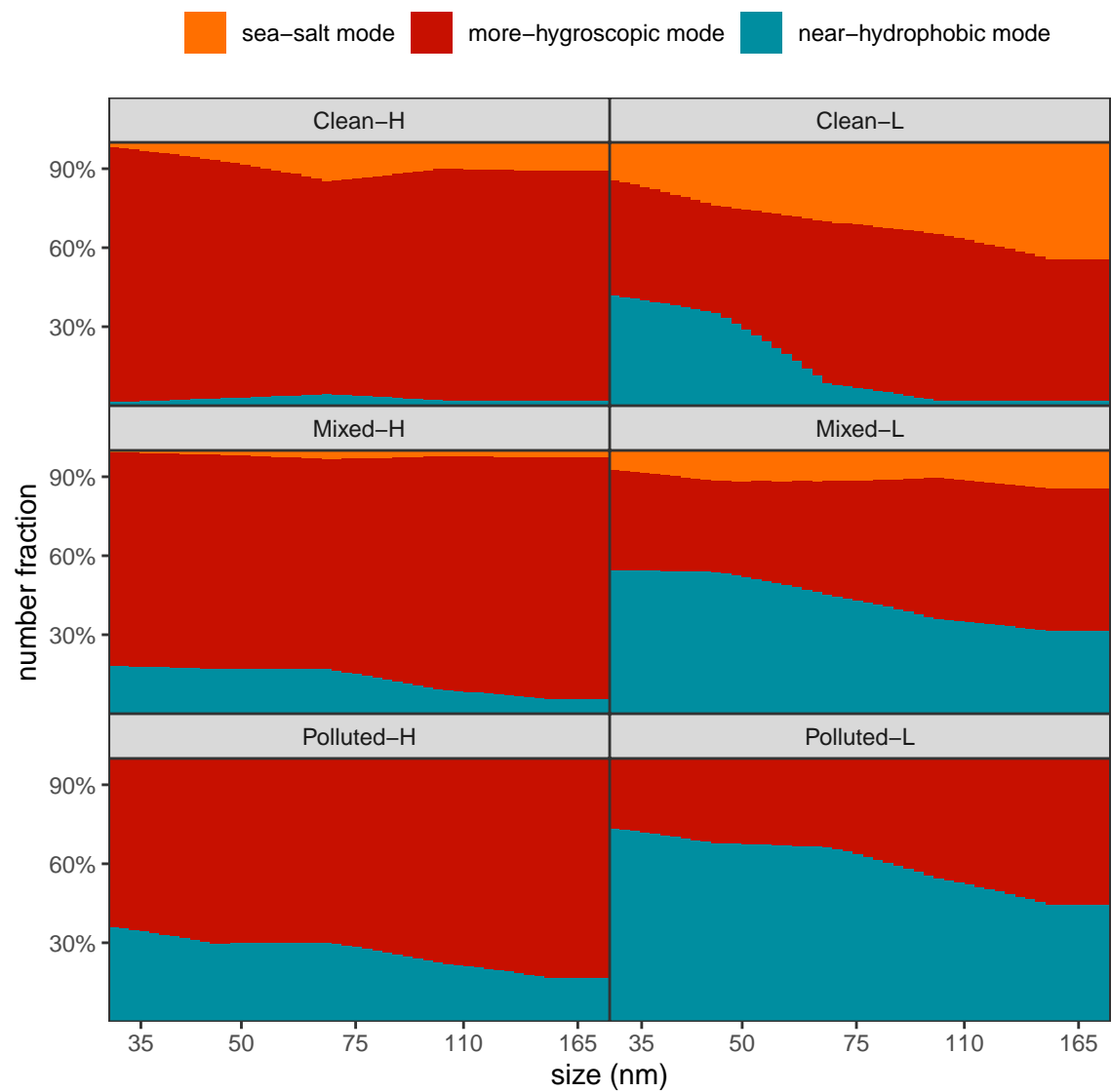


Figure S8. The size resolved number fractions of near-hydrophobic (NH, blue), more-hygroscopic (MH, red) and sea-salt (SS, orange) modes for different types of air masses used in method D.

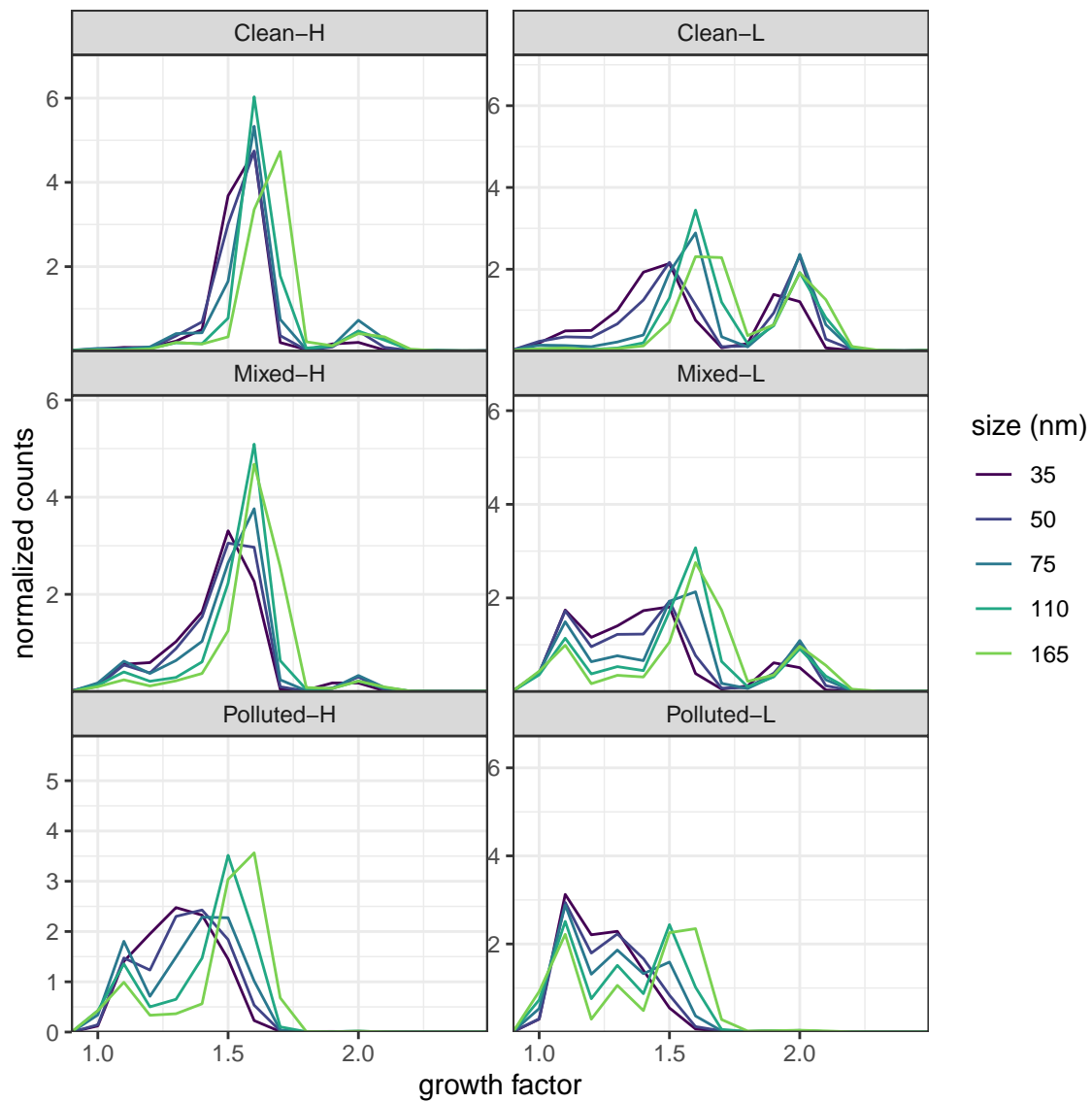


Figure S9. The averaged growth-factor probability density function for different types of air masses.